Novel Three-Phase CM/DM Conducted Emission Separator

Marcelo Lobo Heldwein, *Member, IEEE*, Jürgen Biela, *Member, IEEE*, Hans Ertl, *Member, IEEE*, Thomas Nussbaumer, *Member, IEEE*, and Johann W. Kolar, *Senior Member, IEEE*

Abstract—This paper presents two novel three-phase common-mode (CM)/differential-mode (DM) noise separation networks, which are passive and active networks, to be used in electromagnetic compatibility conducted emission (CE) measurements of three-phase equipment. The passive network is analyzed theoretically, and a prototype is constructed and tested. Its evaluation is presented through frequency response measurements and CE tests performed on a three-phase motor drive and verifies that the network is capable of separating the CM and DM information in a CE measurement condition.

Index Terms—Conducted emissions (CEs), electromagnetic compatibility (EMC) measurements, EMC test setup, noise separator.

I. INTRODUCTION

THREE-PHASE conducted emission (CE) measurements are a major issue for developing high-power electronic equipment that is connected to an electric power grid due to electromagnetic compatibility (EMC) concerns which are reflected in international and regional product regulations. Three-phase power electronic systems, such as motor drives and high power rectifiers, must comply with these regulations. To achieve EMC compliance, electronic equipment must include filtering and/or other electromagnetic emission control strategies.

The development and dimensioning of these emission control techniques are being increasingly investigated, and as a result, analytical, such as presented in [1]–[5], and experimental tools are being developed to support the electrical design engineers. There, the qualitative and quantitative assessment of the noise modes—common mode (CM) or differential mode (DM)—is of great importance since they significantly influence the emission control strategy (e.g., CM or DM filter). Therefore, a device that can be integrated in a three-phase CE standard measurement system and that enables the separate evaluation of CM and DM emission levels is presented in this paper. This device is called three-phase CM/DM noise separator in the following.

Circuits enabling the distinction of noise modes for single-phase systems have been presented in [3]–[13], and their operating principle is based on the fact that summing and subtracting of two sensed voltages directly lead to CM and/or DM emissions. Other methods that apply mathematical analysis through fast Fourier transformation [14] have also been proposed. There, it is important that sampling rates are high enough and phase information is computed correctly, which usually leads to expensive or inaccurate measurements.

A three-phase measurement system capable of separately measuring both noise modes is proposed in [15]. It employs current transducers and hybrid junctions [15]. However, this system does not fulfill all the specifications of CISPR 16, and it requires a complex assembly for the test setup. In [14], another measurement technique is presented, which is suitable for high power levels, but it does not use a line impedance stabilization network (LISN) and needs numerical treatment for the acquired data. Numerical models are presented in [16], which also allow CM and DM emission level estimation but only if a detailed model of the system is available. Another method is given in [17], which uses postmathematical processing in order to calculate the CM/DM emission values based on the noise propagation characteristics for the converter under consideration.

In order to overcome the mentioned limitations, a novel measurement hardware, which is inserted between the three-phase LISN and the EMC test receiver, is proposed in this paper. This hardware enables a real-time direct measurement of DM and CM emission levels in a typical CISPR 16 specified setup [18]–[20].

In Section II, a short discussion on CE measurements in three-phase systems and the mathematical relationships between measured voltages and noise modes are presented. This provides the analytical basis for the CM/DM separation in three-phase systems. Two basic circuit topologies for three-phase CM/DM separation networks—passive- and active-component-based ones—are proposed in Section III. There, only the passive topology is analyzed in detail for the sake of brevity. Details of the active circuit can be found in [21]. A hardware realization of the passive circuit is discussed in Section IV, and experimental results, illustrating the performance of the hardware prototype, are given in Section V.

II. REVIEW OF THREE-PHASE CE MEASUREMENTS AND NOISE COMPONENTS

In order to obtain noise measurements, which are comparable to measurements under different line conditions and which
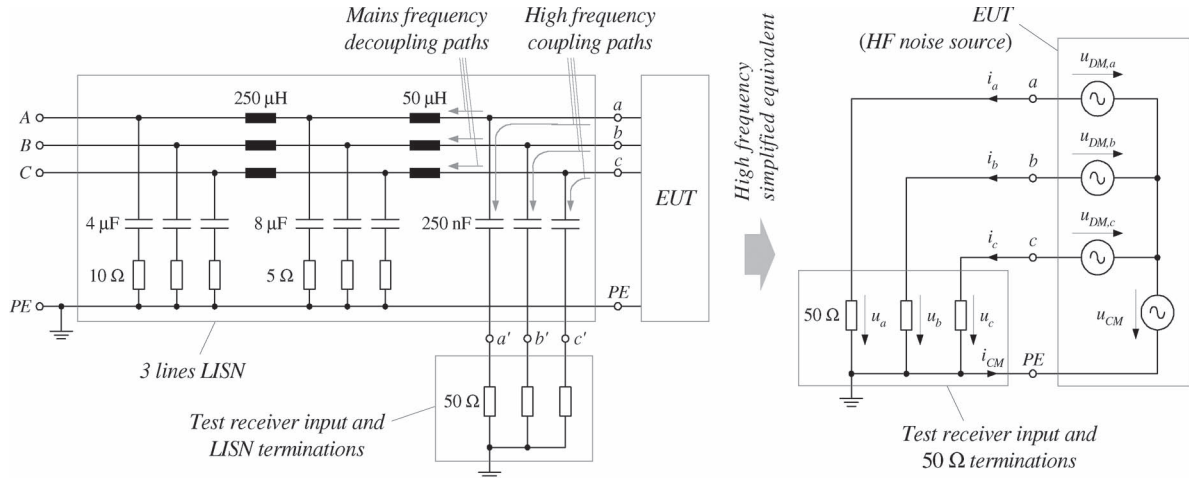
Fig. 1.   Typical three-phase CE compliant measurement setup schematic and HF equivalent circuit.

comply to CE standards, an LISN has to be utilized. There, the LISN basically has to fulfill the following three functions: 1) Define the mains impedance in order to standardize the measurement; 2) decouple the low frequency ac power supply voltage from the measurement equipment; and 3) provide a high frequency (HF) coupling path between the equipment under test (EUT) and the measurement test receiver.

The impedance curve of an LISN is defined in the EMC standards, for instance, in CISPR 16 [20]. A typical realization of a three-phase LISN circuit is shown in Fig. 1 along with a simplified HF equivalent circuit (cf. Fig. 1). For the CE measurement process, a test receiver with 50-Ω input impedance is connected to one of the LISN channels while the remaining two LISN ports are terminated with a 50-Ω resistor providing a symmetric measurement condition.

Assuming an ideal decoupling of the EUT from the mains and a perfect coupling to the test receiver at high frequencies (> 150 kHz), the circuit shown in Fig. 1 could be simplified to the HF equivalent circuit shown in the left side of Fig. 1. There, the input ports a, b, and c of the EUT are directly connected to the input ports of the test receiver and all HF noises from the EUT are directly coupled to the test receiver, while the mains ports A, B, and C are separated from the EUT.

The measured voltages u_i $(i = a, b, c)$ at the test receiver 50-Ω sensing resistors (cf. Fig. 1) consist of DM and CM components

$$u_i = u_{DM,i} + u_{CM}. \tag{1}$$

These two components are caused by the three DM currents $i_{DM,i}$ and a CM current i_{CM} circulating between the EUT and the test receiver. There, the currents i_i, flowing to the test receiver input ports, are given by

$$i_i = i_{DM,i} + \frac{i_{CM}}{3}. \tag{2}$$

Furthermore, the sum of the DM currents is, per definition, equal to zero, and the sum of the currents flowing to the test receiver is equal to the CM current

$$i_a + i_b + i_c = i_{CM}. \tag{3}$$

Therefore, the CM voltage u_{CM} can be evaluated by the summation of the measured voltages

$$u_a + u_b + u_c = R \cdot (i_a + i_b + i_c) = R \cdot i_{CM} = 3 \cdot u_{CM} \tag{4}$$

where R is the input resistance of the test receiver (typically 50 Ω). For calculating the DM components, the CM part has to be eliminated. This can be achieved by subtracting two test receiver voltages

$$u_a - u_b = u_{DM,a} - u_{DM,b} \tag{5}$$

since $u_i = u_{DM,i} + u_{CM}/3$.

Based on (4) and (5), it is now possible to evaluate the CM and DM components separately, as will be shown in the following section.

III. THREE-PHASE NOISE SEPARATION NETWORKS

In order to practically implement the mathematical formulation given in the previous section and properly separate both noise modes, two circuit topologies are proposed in Fig. 2 [21]. There, the HF noise components are depicted by a CM voltage source u_{CM} and three DM voltage sources $u_{DM,a}$, $u_{DM,b}$, and $u_{DM,c}$.

In Fig. 2(a), a purely passive solution with three transformers in Y/Δ-connection is shown, which will be analyzed in detail as follows. The active circuit given in Fig. 2(b) builds the CM voltage by adding all three input voltages and dividing the sum by three (4). Then, the DM voltage could be calculated by subtracting the CM voltage from the measured voltage by using operational amplifiers. In order to obtain good HF results, amplifiers with very large bandwidths and high power supply rejection ratios are required. Furthermore, the active solution requires a galvanically insulated power supply with low capacitive coupling to ground/mains, which increases costs. However, the active solution would provide well-defined input impedances and a good control of the insertion loss, allowing an easy compensation.

Because of the mentioned disadvantages of the active solution and the simplicity of the passive one, the focus is put on the
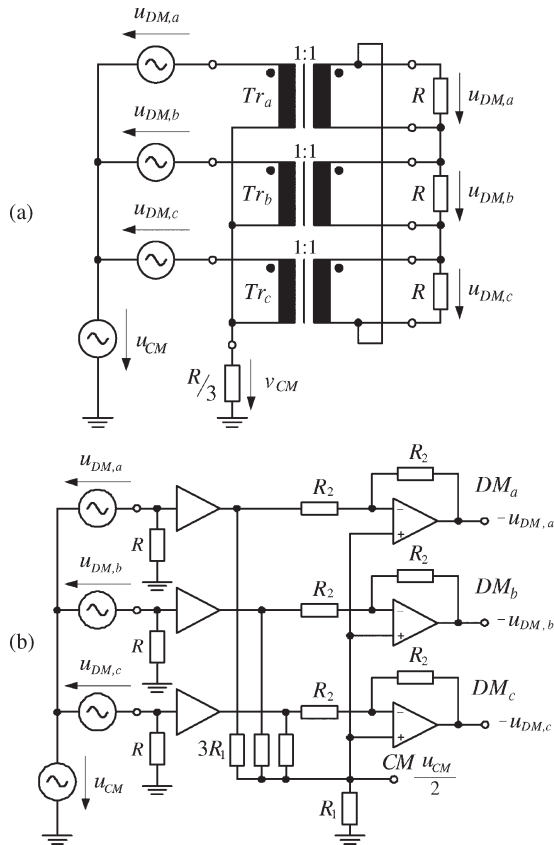
Fig. 2. Three-phase CM/DM noise separator proposals [21]. (a) Passive solution. (b) Active solution.

passive solution in the following. Further details on an active separator can be found in [21].

In the next step, the ideal passive separator is analyzed theoretically, and thereafter, the influence of parasitic elements of the passive components is investigated.

A. Analysis of the Passive Noise Separator

The passive solution shown in Fig. 2(a) mainly consists of three transformers Tr_a, Tr_b, and Tr_c with star-connected primaries, delta-connected secondary windings, and a one-to-one turns ratio. The primary side star point is connected to the ground via a resistor $R/3$, while the secondary windings are terminated by resistors with the value R.

The CM voltage is built by adding the three currents coming from the EUT (4). Due to the Y/Δ-connection of the transformers, the CM current on the primary side, which is equal in all three transformers/phases, flows on the secondary side in the triangle of the Δ-connection and not via the DM resistors (cf. Fig. 3(a) and Fig. 5). Therefore, the CM current does not cause a voltage drop on the secondary side (the Δ-connection acts like a short circuit in the zero sequence system), and only the DM current, which must flow via the resistors on the secondary side, causes a voltage drop [cf. Fig. 3(b)].

This behavior also could be determined by mathematical analysis of the circuit, which will be explained in the following for
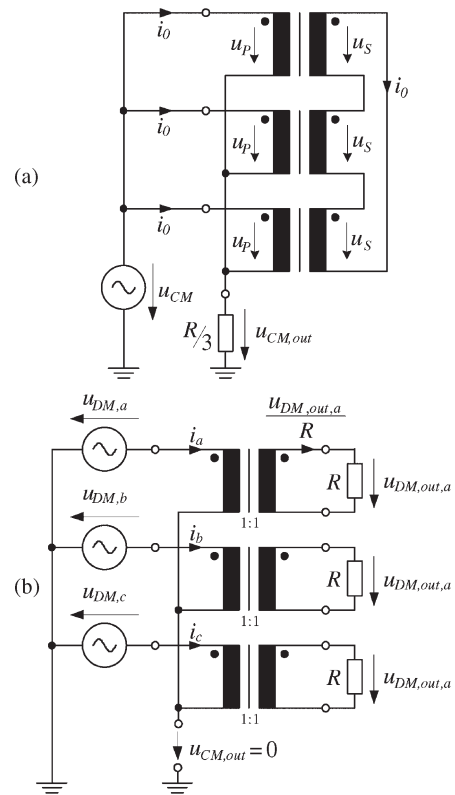

Fig. 3. Simplified equivalent circuits of the noise separator shown in Fig. 2(a) for (a) CM and (b) DM in the case of symmetric components/design (i.e., $u_{\text{DM},a} + u_{\text{DM},b} + u_{\text{DM},c} = 0 \rightarrow i_a + i_b + i_c = 0$).

further clarifying the noise separation. First, the mesh equation

$$u_{\text{CM}} + u_{\text{DM},i} - u_{\text{DM,out},i} = u_{\text{CM,out}} \tag{6}$$

is set up [cf. Fig. 2(a)]. There, the DM output voltage $u_{\text{DM,out},i}$ has been transferred to the primary. Due to the Δ-connection on the secondary side, the sum of the DM voltages at the output must be zero

$$\sum_{i-1}^{3} u_{\text{DM,out},i} = 0. \tag{7}$$

Furthermore, the sum of the DM voltage sources $u_{\text{DM},i}$ must be zero due to their definition

$$\sum_{i-1}^{3} u_{\text{DM},i} = 0. \tag{8}$$

This leads to

$$u_{\text{CM}} = u_{\text{CM,out}} \tag{9}$$

which results by summing the three equations (6) ($i = a, b, c$), inserting (7) and (8), and dividing the result by three.

With (9), the CM voltage $U_{\text{CM,out}}$ in (6) could be replaced by u_{CM}. This results in

$$u_{\text{DM},i} = u_{\text{DM,out},i}. \tag{10}$$

Therefore, the proposed network perfectly separates the CM and DM voltages and provides in its output ports the values for the respective voltages if parasitic elements are neglected.
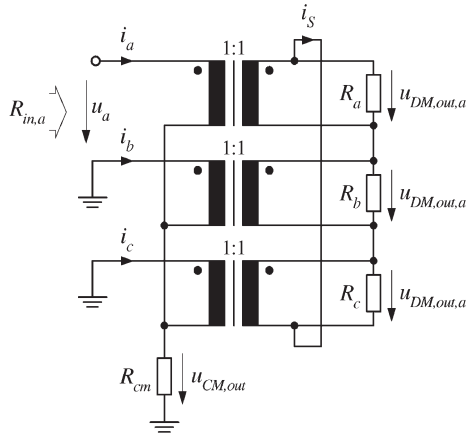
Fig. 4. Circuit used for the calculation of the input impedances to ground (PE).

B. Input Impedance Calculation

Another relevant issue for the measurement setup is the value of the input impedances of the network, since the CE measurements with an LISN usually specify 50-Ω balanced sensing resistors. Since the network is symmetric, the analysis of the input impedances is performed only for input a, as shown in Fig. 4.

Solving the mesh and node equations for the circuit given in Fig. 4 leads to

$$\frac{u_a}{i_a} = 9 \cdot \frac{R_a \cdot R_b \cdot R_c \cdot R_{\mathrm{CM}}}{R_a \cdot R_b \cdot R_c + R_{\mathrm{CM}} \cdot [4 \cdot R_b \cdot R_c + R_a \cdot (R_b + R_c)]} \cdot \tag{11}$$

There, the resistors R_i $(i = a, b, c)$ must be made equal for a balanced circuit

$$R_a = R_b = R_c = R. \tag{12}$$

Replacing (12) in (11) results in

$$R_{\mathrm{in},a} = \frac{u_a}{i_a} = \frac{9}{\frac{6}{R} + \frac{1}{R_{\mathrm{CM}}}}. \tag{13}$$

In order not to modify the test setup, the input resistance $R_{\mathrm{in},a}$ of the noise separator should have the same value as the input resistance of the test receiver (typically equal to 50 Ω), i.e., $R_{\mathrm{in},i} = R = 50$ Ω. With this relation, (13) could be solved as

$$R_{\mathrm{CM}} = \frac{R}{3}. \tag{14}$$

Thus, the CM measurement resistor R_{CM} must be one third of the test receiver's input resistance in order not to influence the standard CE measurement setup.

C. Influence of Parasitic Elements on the Performance of the Noise Separator

In the previous sections, it has been shown that the ideal noise separator can perfectly separate CM and DM noises without impairing the measurement setup. In the next step, the impact
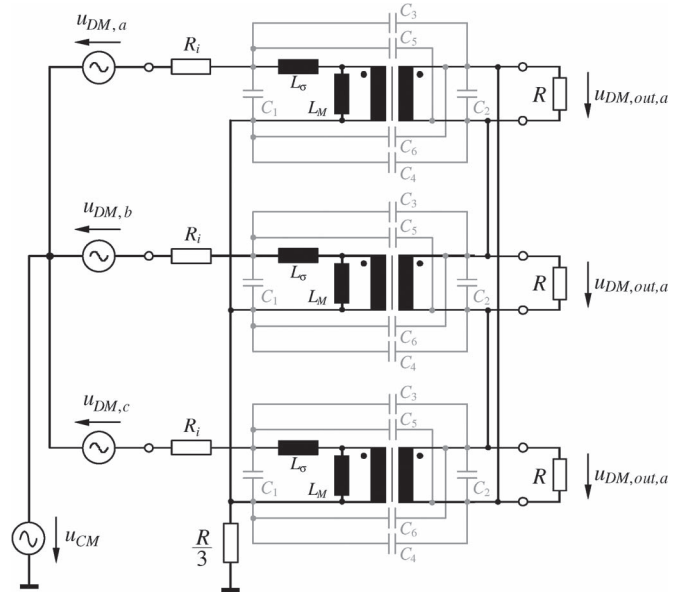

Fig. 5. Circuit used for the parasitic elements analysis of the three-phase CM/DM noise separator.

of parasitic elements on the noise separation is investigated based on the circuit shown in Fig. 5. There, the transformer has been replaced by an equivalent circuit, which accounts for the leakage (L_σ) and magnetizing (L_M) inductances, as well as for the parasitic capacitances ($C_1 \ldots C_6$) [23]. For simplification, the leakage inductance is concentrated on the primary side only.

The influence of the mentioned parasitic elements could be described by the following characteristics: 1) DM transmission ratio (DMTR); 2) CM transmission ratio (CMTR); 3) DM rejection ratio (DMRR); 4) CM rejection ratio (CMRR); and 5) input impedance (Z_{in}) seen from one of the input terminals to protective earth (PE). These are defined in (15)–(19), shown at the bottom of the next page.

With these definitions, the key parasitic elements influencing the transmission/rejection of the noise separator are discussed. First, a purely CM excitation, as shown in Fig. 6, is considered. There, also the current distribution for a symmetric system, i.e., all three transformers are identical, is shown, and it could be seen that the Δ-connection on the secondary side acts as short circuit for the CM excitation.

For the CMTR, the DM voltage noise sources $u_{\mathrm{DM},i}$ are zero, so that the three input ports build a short circuit, the three primary sides are connected in parallel, and the equivalent circuit could be simplified to the circuit shown on the lower portion of Fig. 6. The CM current flows via the three transformers and the short circuit on the secondary side to the CM output $u_{\mathrm{CM,out}}$ with $R/3$. There, the parallel resonant circuit consisting of the leakage inductance and the parasitic transformer capacitances, which build a voltage divider with the output resistance, causes a significant distortion of the CMTR around the resonance frequency. An asymmetric circuit, i.e., which the three transformers have different parasitic elements, does not basically influence the CMTR very much, since the three transformers are connected in parallel for the CMTR. Only a leakage inductance in the Δ-connection increases the
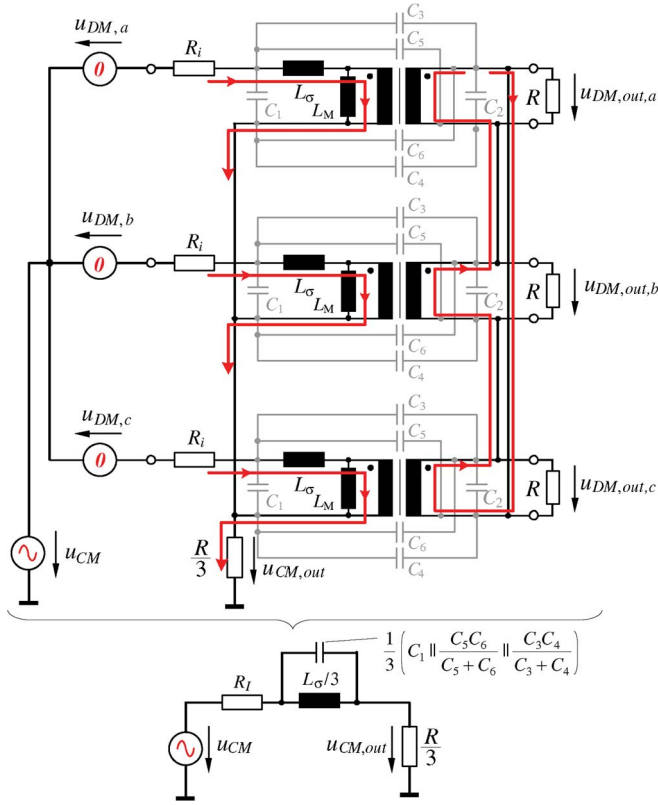
Fig. 6. Current flow with purely CM excitation ($i_{\mathrm{DM}} = 0$) for determining the influence of parasitic elements L_σ, L_M, and $C_1 - C_6$ on the CM transfer and rejection function (CMTR/CMRR).

deviation in the CMTR, since it is in the current path between the voltage source u_{CM} and the output $u_{\mathrm{CM,out}}$, and it resonates with the parasitic capacitances of the transformer.

With a purely symmetric circuit, the CMRR is zero, i.e., the CM excitation does not cause any DM voltage at the output due to the Δ-connection. In case the short circuit due to the Δ-connection is not ideal, a significant voltage value at the three DM outputs results. If a small inductance L_Δ in the Δ-connection is assumed, the DM voltage rises with frequency since the impedance of the "short circuit" increases, until a resonance between the inductance L_Δ and the capacitances
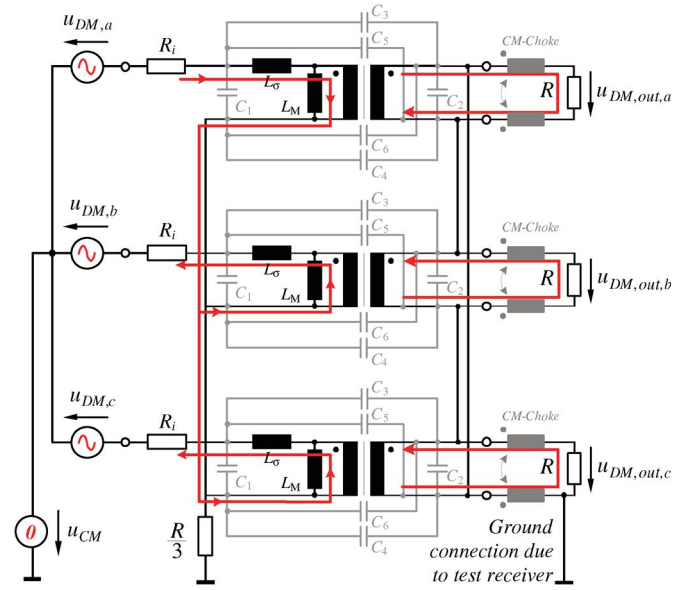

Fig. 7. Current flow with purely DM excitation ($CM = 0$) for determining the influence of the parasitic elements L_σ, L_M, and $C_1 - C_6$ on the DM transfer and rejection function (DMTR/DMRR).

C_3 and C_5 occurs. Aside from the inductance L_Δ, also an asymmetric circuit causes DM voltages since the common currents in the three transformers are not equal, which is required for the Δ-connection to be effective as short circuit for DM. There, particularly an asymmetric leakage inductance or asymmetric capacitances $C_3 \ldots C_6$ (interwinding capacitances) lead to a large DM output voltage at higher frequencies for purely CM input voltage. Consequently, it is very important for the CMTR [cf. Fig. 9(a)] and the CMRR [cf. Fig. 9(b)] that the three transformers have the same parasitic values, i.e., the circuit is symmetric, and that the Δ-connection on the secondary side has a very small inductance.

After the CM functions, a purely DM excitation is considered, as shown in Fig. 7. There, it is important to note that, due to the measurement receiver, one of the DM outputs is grounded. This leads to an asymmetric circuit and influences the DMTR and DMRR. Connecting all three DM outputs

$$DMTR = 20 \log \left(\left| \frac{U_{\mathrm{DM,out},A}}{U_{\mathrm{DM},a}} \right| \right) \Bigg|_{U_{\mathrm{DM},b}=U_{\mathrm{DM},a} \cdot \mathrm{e}^{j\frac{2\pi}{3}}, U_{\mathrm{DM},c}=U_{\mathrm{DM},a} \cdot \mathrm{e}^{-j\frac{2\pi}{3}}, U_{\mathrm{CM}}=0} \tag{15}$$

$$CMTR = 20 \log \left(\left| \frac{U_{\mathrm{CM,out}}}{U_{\mathrm{CM}}} \right| \right) \Bigg|_{U_{\mathrm{DM},a}=U_{\mathrm{DM},b}=U_{\mathrm{DM},c}=0} \tag{16}$$

$$DMRR = 20 \log \left(\left| \frac{U_{\mathrm{CM,out}}}{U_{\mathrm{DM},a}} \right| \right) \Bigg|_{U_{\mathrm{DM},b}=U_{\mathrm{DM},a} \cdot \mathrm{e}^{j\frac{2\pi}{3}}, U_{\mathrm{DM},c}=U_{\mathrm{DM},a} \cdot \mathrm{e}^{-j\frac{2\pi}{3}}, U_{\mathrm{CM}}=0} \tag{17}$$

$$CMRR = 20 \log \left(\left| \frac{U_{\mathrm{DM,out},A}}{U_{\mathrm{CM}}} \right| \right) \Bigg|_{U_{\mathrm{DM},a}=U_{\mathrm{DM},b}=U_{\mathrm{DM},c}=0} \tag{18}$$

$$Z_{\mathrm{in}} = \frac{U_{\mathrm{DM},a}}{I_{\mathrm{DM},a}} \Bigg|_{U_{\mathrm{DM},b}=U_{\mathrm{DM},a} \cdot \mathrm{e}^{j\frac{2\pi}{3}}, U_{\mathrm{DM},c}=U_{\mathrm{DM},a} \cdot \mathrm{e}^{-j\frac{2\pi}{3}}, U_{\mathrm{CM}}=0} \tag{19}$$
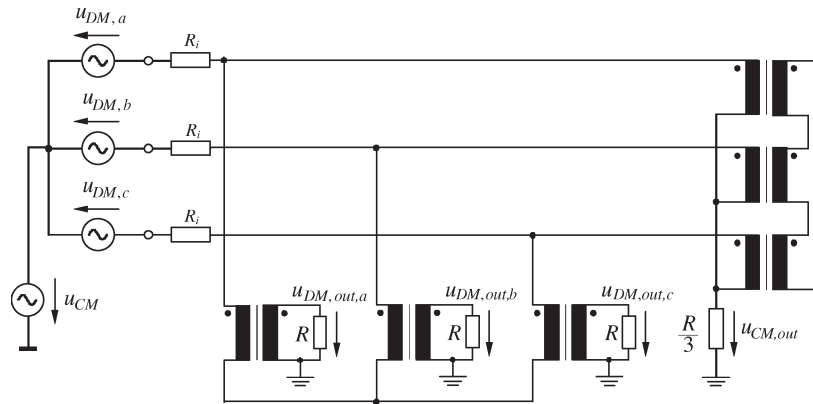
Fig. 8.   Two-stage noise separator, which is basically more symmetric than the design shown in Fig. 6 but increases the parasitic elements significantly.

to ground is not possible, since this would short-circuit the secondary side completely, due to the Δ-connection. Only a realization of the CM/DM noise separation by two stages with six instead of three transformers, as shown in Fig. 8, would avoid the problem but leads to more parasitic elements. There, the CMRR could be improved by inserting a three-phase CM choke between the noise source and the three transformers for the DM outputs.

Due to the asymmetric circuit because of the ground connection and due to the parasitic interwinding capacitances $C_3 \ldots C_6$, the DMRR basically could not be zero. In order to reduce the influence of the ground connection, a CM choke could be inserted at the DM outputs. There, it is very important that the leakage inductance of the CM chokes is very small, since it is connected in series to the output resistors and directly influences the DMTR.

In the case of asymmetric parameters of the three transformers, the DMRR is deteriorated further. The reason for this is that, in this case, due to the nonequal impedances of the transformers, the symmetric input voltages $u_{DM,i}$ excite not only DM currents but also a CM current, since the sum of the currents is no longer zero. There, an asymmetric leakage inductance has the strongest influence on the DMRR [cf. Fig. 9(d)] in the lower frequency range, and the parasitic input/output capacitances affect mainly the higher frequency range.

Asymmetric leakage inductances have also a strong influence on the DMTR [cf. Fig. 9(c)], since the leakage inductance and the output resistance R_{DM} build voltage dividers. The influence of the parasitic capacitances is relatively small. These mainly determine the resonance frequency of the parallel resonant circuit $L_\sigma \| (C_3, C_4, C_5, C_6)$, which affects the upper frequency range (typically above 30 MHz).

Aside from the parasitic elements of the passive components, also the inner resistance of the voltage sources modeled by R_i has an effect on the noise separation. Potential unbalances between the symmetric circuit components (e.g., $R_i, i = a, b, c$) have similar effects as an unbalance of the leakage inductance of the transformer, since a symmetric DM voltage will cause an asymmetric current, i.e., also a CM current is excited.

Finally, also the input impedance of the separator is significantly influenced by the symmetry of the circuit. In the case of a DM-noise measurement with one DM output grounded, the three input impedances of the separator deviate from each other in the range of higher frequencies, as shown in Fig. 9(e). Moreover, also asymmetric values of the transformer parasitic increase the deviation of the input impedance from its ideal value.

IV. THREE-PHASE NOISE SEPARATOR REALIZATION

In order to verify the presented theoretical results, a three-phase CM/DM noise separator, whose schematic is shown in Fig. 10 and the corresponding photo in Fig. 11, has been built. This separator is specified to be used in a standard CISPR 16 CE test setup using a typical $(50 \ \mu H + 5 \ \Omega) // 50 \ \Omega$ V-network LISN and applying input line-to-line voltages of 400 V/50 Hz.

The prototype consists of three transformers Tr_a, Tr_b, and Tr_c and three CM inductors L_a, L_b, and L_c. Furthermore, $R = 50 \ \Omega$ is employed, which ensures an equivalent resistance of the noise separator inputs to ground of 50 Ω and allows the measurement of the CM and DM noise voltages directly from the respective output ports. For measuring a DM-noise voltage, the corresponding output is connected to the input of the test receiver (input impedance of 50 Ω) after removing the output resistor R, which consists of a 50-Ω British Naval Connector termination. The CM noise could be measured at the CM output. There, two 50-Ω resistors must be connected in parallel to the test receiver input in order to obtain the desired CM termination resistor $R/3$.

A. Design of the Noise Separator

For building a noise separator, three single-phase transformers and three CM inductors are required, which have good HF behavior. In order to avoid saturation, the core area of the transformer must be adapted to the volt seconds of the transformer input voltage. This volt seconds is mainly determined by the low frequency (50/60 Hz) components of the DM LISN output voltage, due to the low frequency and relatively high amplitude. The CM LISN output voltage does not significantly influence the flux in the core since the Δ-connection on the secondary side acts like a short circuit in the zero sequence system, so that the voltage drop across the windings is ideally zero in the zero sequence system.

In Fig. 12, the LISN DM output voltage for a 5-kW rectifier system operating at 20 kHz without input filter is shown as
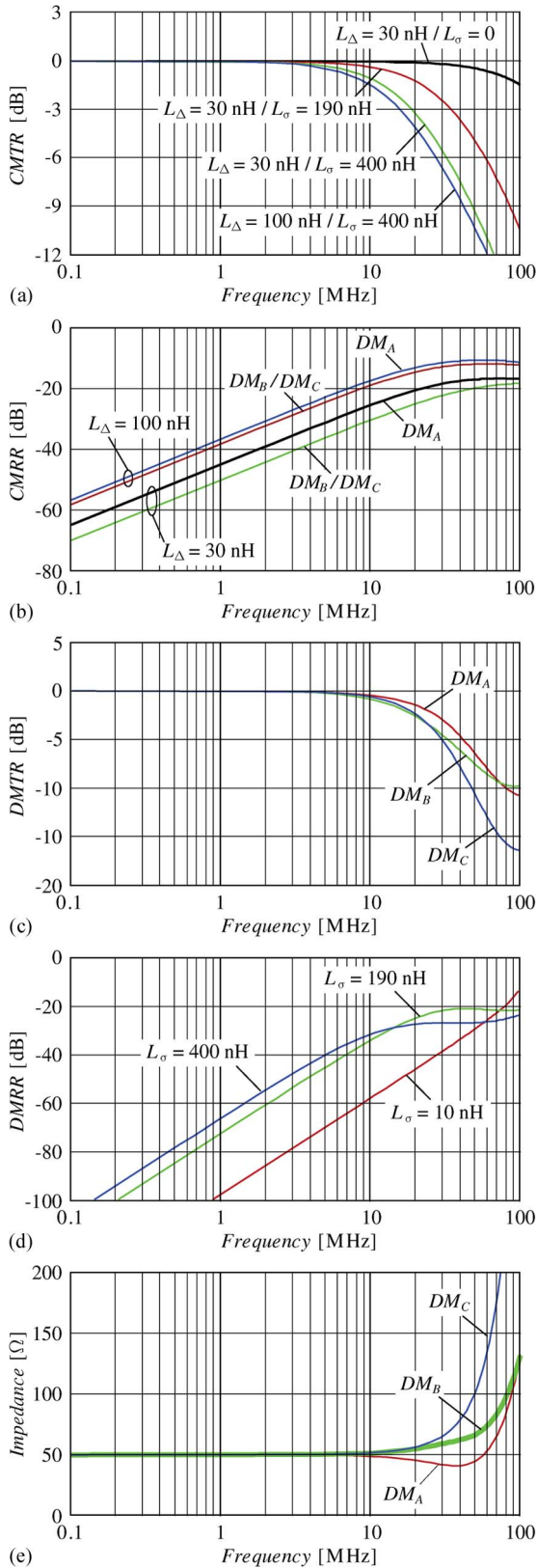
Fig. 9. Influence of parasitic elements on the performance of the separation network. Values if not specified differently: $C_1 = C_2 = -11.6$ pF, $C_3 = C_4 = 13.4$ pF, $C_5 = C_6 = 13.1$ pF, $L = 10$ mH, $L_\sigma = 190$ nH, $L_{cm} = 0$, and $R = R_i = 50$ Ω. Shown: (a) CMTR as function of leakage inductance and inductance in the Δ-connection; (b) CMRR for the DM outputs for different values of inductance in the Δ-connection; (c) DMTR for the different DM outputs; (d) DMRR for three different values of the leakage inductance $L\sigma = 10$, 190, and 400 nH; and (e) input impedance for the inputs.
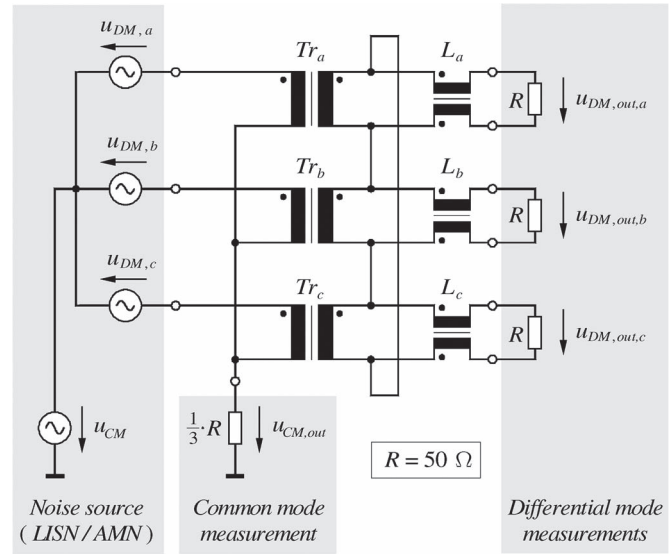

Fig. 10. Circuit schematic of the three-phase CM/DM noise separator prototype.

Fig. 11. Three-phase CM/DM separator prototype photograph. Overall dimensions: $7.0 \times 7.0 \times 8.2$ cm ($2.8 \times 2.8 \times 3.2$ in).
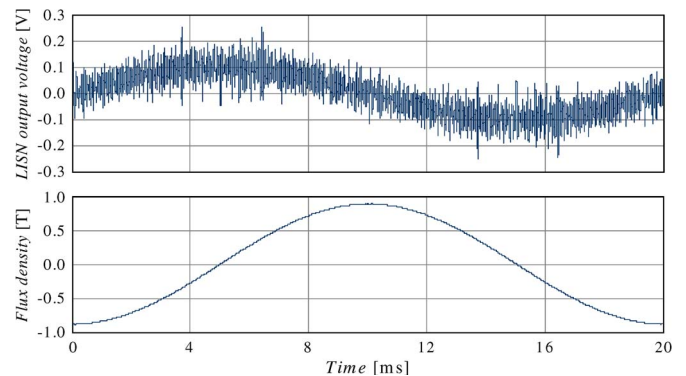

Fig. 12. Calculated flux density in the designed transformers Tr_a, Tr_b, and Tr_c, for a simulated LISN output voltage when feeding a three-phase 5-kW rectifier.

an example. In addition, also the corresponding flux density in the transformer cores is given. There, the specifications of a Vaccumschmelze GmbH (VAC) $25 \times 16 \times 10$-T6000-6-L2025-W380 core made of VITROPERM ($B_{Sat} \approx 1.2$ T) from VAC and a winding with 10:10 turns have been assumed. In the considered case, the peak value of the flux density remains well below the saturation value, but this could vary in dependence

of the application. In case the input voltage would cause a saturation of the core, an attenuator could be inserted between the LISN and the noise separator. This could also be used for testing whether the cores are close to saturation: If the spectrums with and without attenuator are approximately the same, the core is not close to saturation.

Aside from the basic transformer function, particularly the parasitic elements are important. There, the leakage inductance must be as small as possible in order not to deteriorate the transfer functions DMTR and CMTR. Furthermore, the parasitic capacitance between primary and secondary should be small, in order to prevent CM paths between primary and secondary, which influences the CMRR. Furthermore, the parameters should be stable and reproducible, so that a separator with symmetric components with respect to the three phases could be achieved.

The CM chokes in the separator prototype are built with a VAC 12.5 × 10 × 5-T600-6-L2012-W498 core, which also consists of VITROPERM 500 F but is significantly smaller than the transformer core. The winding has two times ten turns. This setup results in a CM inductance of 1 mH and a resonance frequency of 30 MHz.

Remark: For applying the separator, a three- or four-line LISN must allow simultaneous access to all three-phase output ports. In case this is not possible, three individual single-phase LISNs could be employed. All asymmetries presented in the test circuit composed of the LISN and the noise separator will influence the measurements, particularly in the higher frequency range, and should be avoided.

V. EXPERIMENTAL EVALUATION

Some of the frequency response characteristics of the prototype were measured with an impedance and a network analyzer. These measurements were performed with 50-Ω input and output impedances. The most significant results of these measurements are shown in Figs. 13 and 15, while the test setups employed in the measurements are shown in Fig. 14. As the noise separator is intended to discriminate CM and DM, it is important to check how good the attenuation of the other noise components is, for instance, when measuring a CM signal, the influence of the DM channels is needed to be known. This can be evaluated through the measurement of the DMRR of all channels and CMRR for the DM channels. The DMRRs of the CM port are shown in Fig. 13(a), and for all cases, it is higher than 70 dB at 150 kHz and higher than 25 dB up to 30 MHz. The DMTR curves for the three DM channels are quite similar, and only one is shown in Fig. 13(b), where the presented −3-dB cutoff frequency is higher than 20 MHz and good symmetry among the channels is observed. The CMRR of the DM output ports is shown in Fig. 13(c), showing around 50 dB in the lower frequency range and being around 20 dB at 10 MHz. In Fig. 13(d), the insertion loss between the measured CM output voltage and a CM input signal (CMTR) is plotted, and a flatband up to more than 20 MHz is observed. The non-idealities of the circuit also lead to imperfect input impedances (cf., Fig. 15), which increase with increasing frequencies, leading to higher measurement results in the frequency range above
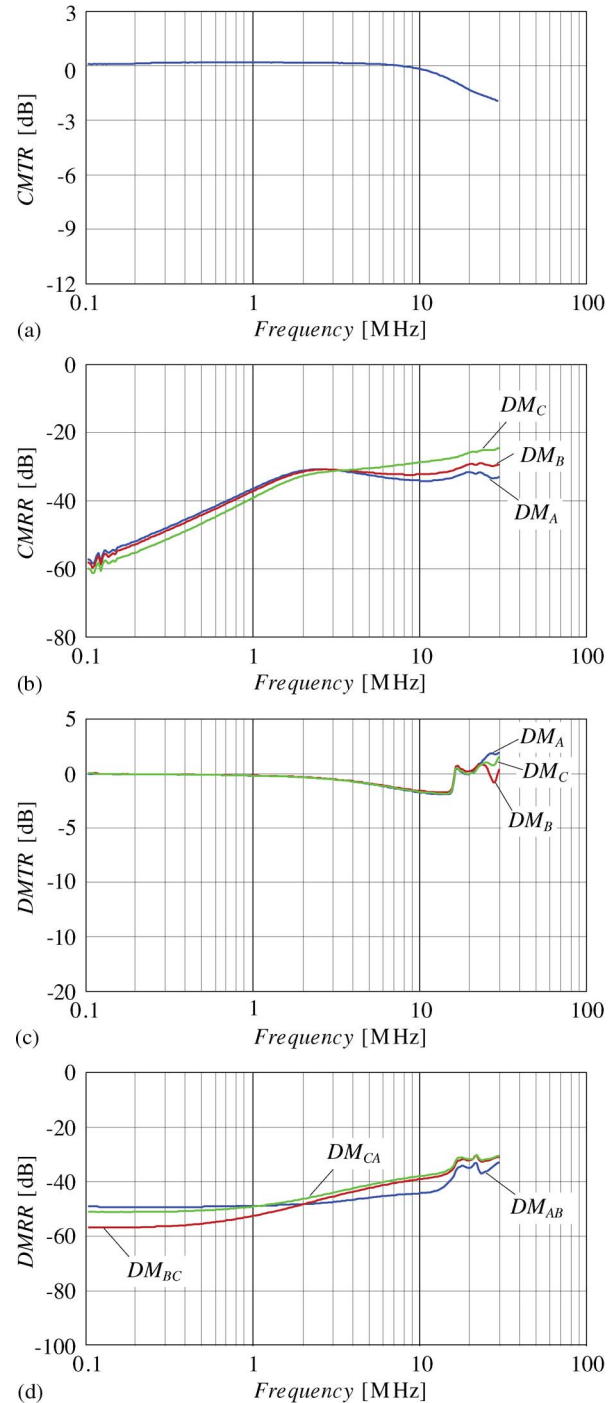

Fig. 13. Measured frequency characteristics for the CM/DM noise separator. (a) DMRR. (b) DMTR. (c) CMRR. (d) CMTR.

10 MHz. The measured frequency characteristics show that the separation network performs better in the frequency range up to 1 MHz. However, rejection ratios on the order of 30 dB are observed at 30 MHz, guaranteeing clear separation of the noise modes.

CE measurements as specified in CISPR 16 were performed by utilizing a setup as shown in Fig. 16 in order to give an example for the use of the three-phase CM/DM separator. The EUT was a regenerative drive feeding a 10-kVA electric motor. The test conditions were as follows: input voltages
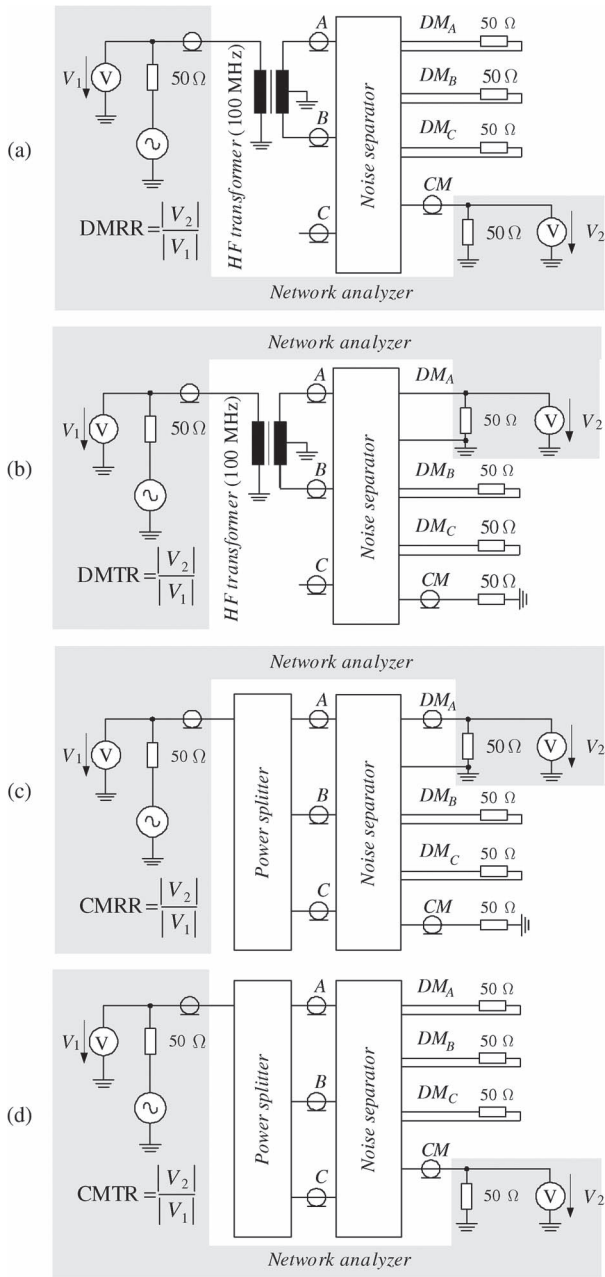
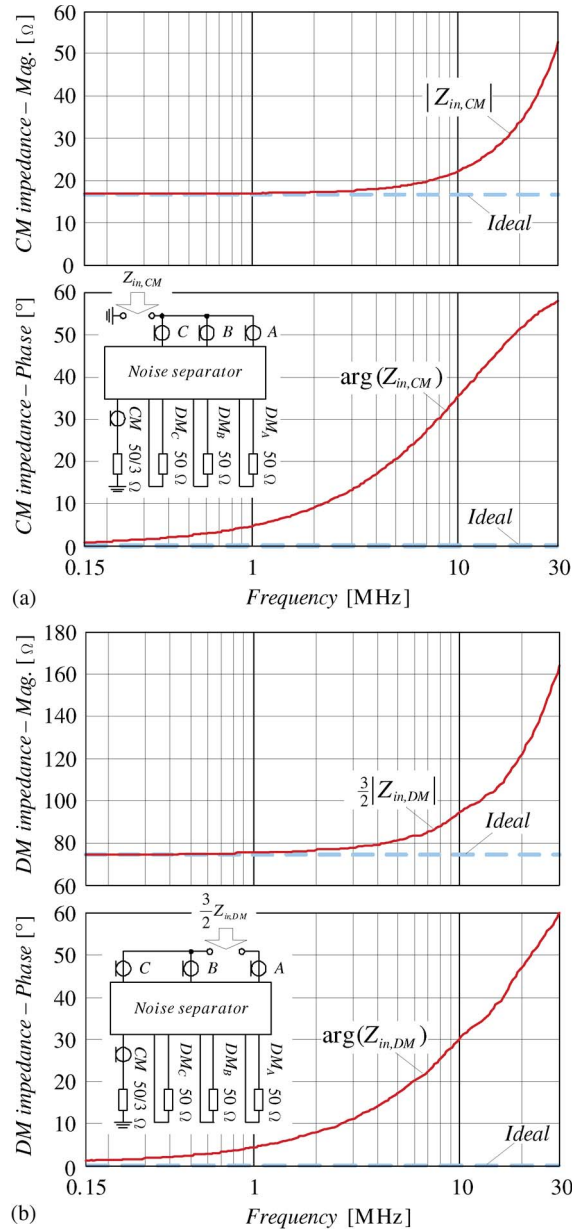Fig. 14. Setups used to measure (a) DMRR, (b) DMTR, (c) CMRR, and (d) CMTR.

Fig. 15. Measured input impedances: (a) Impedance measured from input ports (connected together) to PE and (b) impedance measured between one input port and the other two ports connected together. Ideal values are shown by dashed lines.

$U_{\text{in}} = 400$ V/50 Hz; output power $P_{\text{out}} = 5$ kW. The LISN that conforms with CISPR 16 is constructed to operate from 2 kHz to 30 MHz and is presented in detail in [22]. The access to all output ports is available, thus guaranteeing that the three-phase CM/DM noise separator can be employed.

Fig. 17 shows the acquired data for three measurements done within the same operating conditions, where one is without noise separator Fig. 17(a), the second shows the measured emission levels sensed in one of the DM channels with the presented network Fig. 17(b), and the last one depicts the measurement performed in the CM output port. From the measurements, it is seen that there is a large difference between the levels of DM and CM emissions in the lower frequency range, where the DM emissions are much higher than the CM ones.
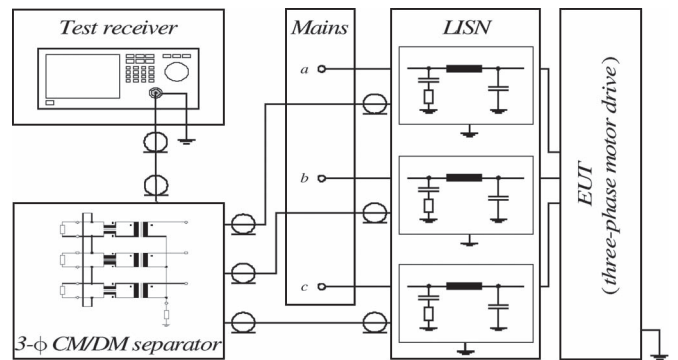

Fig. 16. Test setup for the CE measurements using the proposed three-phase CM/DM noise separation passive network.
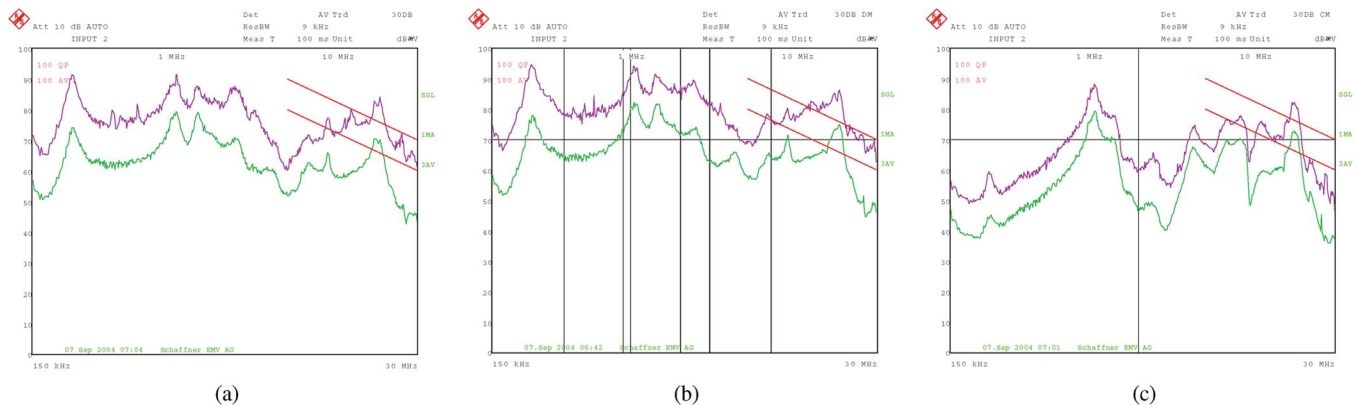
Fig. 17. Measurements performed with and without the noise separator. (Axes) 0 to 100 dB · μV and 150 kHz to 30 MHz. (Upper curves) Quasi-peak measurement as specified in CSIPR 16. (Lower curves) Average detection measurement. (a) Measurements applying directly an LISN. (b) Measurements performed in one noise separator DM output port. (c) Measurements from the noise separator CM output port.

This indicates the necessity of higher DM attenuation at this frequency range. It shows the required attenuation and allows an appropriate filter to be designed. This example shows that the main purpose of the separator, which is acquiring information for filter designs and troubleshooting of power converters, is achieved.

VI. CONCLUSION

This paper has presented two novel three-phase DM/CM separation networks intended to be used in the evaluation of noise sources. The separators' aim is to help in the design and troubleshooting of electromagnetic CE control for electronic equipment. One network is an arrangement of passive components, while the other employs active circuits. The operating principle and characteristics of the passive network were discussed and experimentally verified. CE measurements were successfully performed in a three-phase electric motor drive using the separator indicating the noise levels and dominating modes. This information could be employed to design the CM and DM stages of an EMC filter.

REFERENCES

[1] H. I. Hsieh, J. S. Li, and D. Chen, "Effects of X capacitors on EMI filter effectiveness," *IEEE Trans. Ind. Electron.*, vol. 55, no. 2, pp. 949–955, Feb. 2008.

[2] M. Jin and M. Weiming, "Power converter EMI analysis including IGBT nonlinear switching transient model," *IEEE Trans. Ind. Electron.*, vol. 53, no. 5, pp. 1577–1583, Oct. 2006.

[3] J.-S. Lai, X. Huang, E. Pepa, S. Chen, and T. W. Nehl, "Inverter EMI modeling and simulation methodologies," *IEEE Trans. Ind. Electron.*, vol. 53, no. 3, pp. 736–744, Jun. 2006.

[4] J. Meng, W. Ma, Q. Pan, Z. Zhao, and L. Zhang, "Noise source lumped circuit modeling and identification for power converters," *IEEE Trans. Ind. Electron.*, vol. 53, no. 6, pp. 1853–1861, Dec. 2006.

[5] M. M. Hernando, A. Fernandez, M. Arias, M. Rodriguez, Y. Alvarez, and F. Las-Heras, "EMI radiated noise measurement system using the source reconstruction technique," *IEEE Trans. Ind. Electron.*, vol. 55, no. 9, pp. 3258–3265, Sep. 2008.

[6] C. R. Paul and K. B. Hardin, "Diagnosis and reduction of conducted noise emissions," *IEEE Trans. Electromagn. Compat.*, vol. 30, no. 4, pp. 553–560, Nov. 1988.

[7] M. J. Nave, "A novel differential mode rejection network for conducted emissions diagnostics," in *Proc. IEEE Nat. Symp. Electromagn. Compat.*, 1989, pp. 223–227.

[8] M. J. Nave, *Power Line Filter Design for Switched-Mode Power Supplies.* New York: Van Nostrand Reinhold, 1991.

[9] T. Guo, D. Y. Chen, and F. C. Lee, "Separation of the common-mode- and differential-mode-conducted EMI noise," *IEEE Trans. Power Electron.*, vol. 11, no. 3, pp. 480–488, May 1996.

[10] K. Y. See, "Network for conducted EMI diagnosis," *Electron. Lett.*, vol. 35, no. 17, pp. 1446–1447, Aug. 1999.

[11] S. Wang, F. C. Lee, and W. G. Odendaal, "Characterization, evaluation, and design of noise separator for conducted EMI noise diagnosis," *IEEE Trans. Power Electron.*, vol. 20, no. 4, pp. 974–982, Jul. 2005.

[12] K. Jia, J. Wang, C. Wu, and C. Bi, "A new method for conducted EMI noise diagnosis," in *Proc. 8th Int. Conf. Electron. Meas. Instruments*, 2007, pp. 4-59–4-63.

[13] M. Mardiguian and J. Raimbourg, "An alternate, complementary method for characterizing EMI filters," in *Proc. IEEE Int. Symp. Electromagn. Compat.*, 1999, pp. 882–886.

[14] L. Ran, J. C. Clare, K. J. Bradley, and C. Christopoulos, "Measurement of conducted electromagnetic emissions in PWM motor drive systems without the need for an LISN," *IEEE Trans. Electromagn. Compat.*, vol. 41, no. 1, pp. 50–55, Feb. 1999.

[15] A. De Bonitatibus, C. De Capua, and C. Landi, "A new method for conducted EMI measurements on three phase systems," in *Proc. 17th IEEE Instrum. Meas. Technol. Conf.*, 2000, vol. 1, pp. 461–464.

[16] L. Ran, S. Gokani, J. Clare, K. J. Bradley, and C. Christopoulos, "Conducted electromagnetic emissions in induction motor drive systems. Part I. Time domain analysis and identification of dominant modes," *IEEE Trans. Power Electron.*, vol. 13, no. 4, pp. 757–767, Jul. 1998.

[17] W. Shen, F. Wang, D. Boroyevich, and Y. Liu, "Definition and acquisition of CM and DM EMI noise for general-purpose adjustable speed motor drives," in *Proc. IEEE Power Electron. Spec. Conf.*, 2004, vol. 2, pp. 1028–1033.

[18] T. Nussbaumer, M. L. Heldwein, and J. W. Kolar, "Differential mode input filter design for a three-phase buck-type PWM rectifier based on modeling of the EMC test receiver," *IEEE Trans. Ind. Electron.*, vol. 53, no. 5, pp. 1649–1661, Oct. 2006.

[19] M. L. Heldwein, T. Nussbaumer, and J. W. Kolar, "Differential mode EMC input filter design for three-phase AC–DC–AC sparse matrix PWM converters," in *Proc. IEEE Power Electron. Spec. Conf.*, Aachen, Germany, 2004, pp. 284–291, [CD-ROM].

[20] IEC Int. Special Committee Radio Interference - C.I.S.P.R., C.I.S.P.R. Specification for Radio Interference Measuring Apparatus and Measurement Methods—Publication 16, Geneva, Switzerland, 1977.

[21] J. W. Kolar and H. Ertl, Vorrichtung zur Trennung der Funkstoerspannungen dreiphasiger Stromrichtersysteme in eine Gleich-und eine Gegentaktkomponente, Switzerland, 2004.

[22] F. Beck and W. L. Klampfer, "Measurements of conducted voltage in the low-frequency range from 2 kHz to 30 MHz for high-current industrial applications with regeneration drives," in *Proc. Int. Symp. Electromagn. Compat.*, 2004, vol. 1, pp. 5–10.

[23] J. Biela and J. W. Kolar, "Using transformer parasitics for resonant converters—A review of the calculation of the stray capacitance of transformers," in *Conf. Rec. IEEE IAS Annu. Meeting*, Hong Kong, 2005, pp. 1868–1875.

Marcelo Lobo Heldwein (S'99–M'08) received the B.S. and M.S. degrees in electrical engineering from the Federal University of Santa Catarina, Florianópolis, Brazil, in 1997 and 1999, respectively, and the Ph.D. degree from the Swiss Federal Institute of Technology (ETH), Zürich, Switzerland, in 2007.

He is currently a Postdoctoral Fellow with the Power Electronics Institute, Federal University of Santa Catarina, under the PRODOC/CAPES program, where he was a Research Assistant from 1999 to 2001. From 2001 to 2003, he was an Electrical Design Engineer with Emerson Energy Systems, in São José dos Campos, Brazil, and in Stockholm, Sweden. His research interests include power factor correction techniques, static power converters, and electromagnetic compatibility.

Dr. Heldwein is a member of the Brazilian Power Electronics Society.

Jürgen Biela (S'04–M'06) received the Diploma (with honors) in electrical engineering from the Friedrich-Alexander University, Erlangen, Germany, in 2000, and the Ph.D. degree in electrical engineering from the Swiss Federal Institute of Technology (ETH), Zürich, Switzerland, in 2005. In the course of his M.Sc. studies, he dealt in particular with resonant dc-link inverters at Strathclyde University, Glasgow, U.K., (term project) and the active control of series-connected integrated gate commutated thyristors at the Technical University of Munich, Munich, Germany, (Diploma thesis). In July 2002, he joined the Power Electronic Systems (PES) Laboratory, ETH Zürich, working toward the Ph.D. degree, concentrating on an optimized electromagnetically integrated resonant converter.

He was with the Research Department, A&D Siemens, Germany, from 2000 to 2001, where he focused on inverters with very high switching frequencies, SiC components, and electromagnetic compatibility. From 2006 to 2007, he was a Postdoctoral Fellow with PES and has been a Guest Researcher at the Tokyo Institute of Technology, Tokyo, Japan. Since 2007, he has been a Senior Research Associate with PES, Electrical Engineering Department, ETH Zürich. His current research interests include multidomain modeling, design and optimization of PES, particularly systems for future energy distribution and pulsed power applications, advanced PES based on novel semiconductor technologies, and integrated passive components for ultracompact and ultraefficient converter systems.
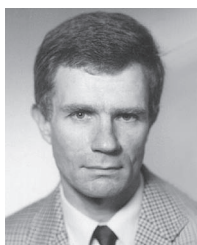
Hans Ertl (M'93) received the Dipl.Ing. (M.Sc.) and Dr.Techn. (Ph.D.) degrees in industrial electronics from the Technische Universität Wien, Vienna, Austria, in 1984 and 1991, respectively.

Since 1984, he has been with the Technische Universität Wien, where he is currently an Associate Professor of power electronics in the Institute of Electrical Drives and Machines. He has performed numerous industrial and scientific research projects in the areas of field-oriented control of ac drive systems, switch-mode power supplies for welding and industrial plasma processes, and active rectifier systems. He is the author or coauthor of numerous scientific papers and patents. His current research activities are focused on switch-mode power amplifiers and multicell topologies, particularly for the generation of testing signals, active ripple current compensators, and several applications in the area of renewable energy systems.

Thomas Nussbaumer (S'02–M'06) was born in Vienna, Austria, in 1975. He received the M.Sc. degree (with honors) in electrical engineering from the University of Technology Vienna, Vienna, Austria, in 2001, and the Ph.D. degree from the Power Electronic Systems (PES) Laboratory, Swiss Federal Institute of Technology (ETH) Zürich, Switzerland, in 2004.

From 2001 to 2006, he was with the PES, where he conducted research on modeling, design, and control of three-phase rectifiers, power factor correction techniques, and electromagnetic compatibility. Since 2006, he has been with Levitronix GmbH, Zürich, Switzerland, where he is currently working on bearingless motors, magnetic levitation, and permanent-magnet motor drives for the semiconductor and biotechnology industry. His current research is focused on compact and high-performance mechatronic systems including novel power electronics topologies, control techniques, drive systems, sensor technologies, electromagnetic interference (EMI), and thermal aspects.

Johann W. Kolar (M'89–SM'04) received the Ph.D. degree (*summa cum laude/promotio sub auspiciis praesidentis rei publicae*) from the University of Technology Vienna, Austria.

Since 1984, he has been an Independent International Consultant in close collaboration with the Vienna University of Technology, in the fields of power electronics, industrial electronics, and high-performance drives. On February 1, 2001, he was appointed as a Professor and Head of the Power Electronic Systems Laboratory, Swiss Federal Institute of Technology (ETH), Zürich, Switzerland. He has proposed numerous novel PWM converter topologies, and modulation and control concepts, e.g., the VIENNA rectifier and the three-phase ac–ac sparse matrix converter. He has published over 300 scientific papers in international journals and conference proceedings. He is the holder of 75 patents. His current research is on ac–ac and ac–dc converter topologies with low effects on the mains, e.g., for power supply of telecommunication systems, more electric aircraft, and distributed power systems in connection with fuel cells. His other main areas of research include the realization of ultracompact intelligent converter modules employing latest power semiconductor technology (SiC), novel concepts for cooling and EMI filtering, multidomain/multiscale modeling and simulation, pulsed power, bearingless motors, and power MEMS.

Dr. Kolar is a member of the Institute of Electrical Engineers of Japan (IEEJ) and the technical program committees of numerous international conferences in the field (e.g., Director of the Power Quality Branch of the International Conference on Power Conversion and Intelligent Motion). From 1997 to 2000, he served as an Associate Editor of the IEEE TRANSACTIONS ON INDUSTRIAL ELECTRONICS, and since 2001, as an Associate Editor of the IEEE TRANSACTIONS ON POWER ELECTRONICS. Since 2002, he has been an Associate Editor for the *Journal of Power Electronics* of the Korean Institute of Power Electronics and a member of the Editorial Advisory Board of the IEEJ *Transactions on Electrical and Electronic Engineering*. He was the recipient of the Best Transactions Paper Award of the IEEE Industrial Electronics Society in 2005 and an Erskine Fellowship from the University of Canterbury, New Zealand, in 2003. In 2006, the European Power Supplies Manufacturers Association awarded the Power Electronics Systems Laboratory of ETH Zürich as the leading academic research institution in Europe.